



Nonlocal Timoshenko representation and analysis of multi-layered functionally graded nanobeams

S. Faroughi¹ · M. S. Sari² · A. Abdelkefi³

Received: 18 June 2020 / Accepted: 18 July 2020 / Published online: 26 July 2020
© Springer-Verlag GmbH Germany, part of Springer Nature 2020

Abstract

The vibration properties of functionally graded multiple nanobeams is studied using Eringen's nonlocal elasticity theory. Beam layers are considered to be continuously connected by layer of linear springs and the nonlocal Timoshenko beam theory is used to model each layer of beam which applies the size dependent effects in FG beam. The material behaviors of FG nanobeams are assumed to vary over the thickness based to the power law. The Hamilton's principle is used to derive the governing differential equations of motion according to Eringen nonlocal theory and a Chebyshev spectral collocation method is employed to convert the coupled equations of motion into algebraic equations. The discretized boundary conditions are applied to adjust the Chebyshev differentiation matrices, and the system of equations is then expressed in the matrix–vector form. Next, the coupled natural frequencies and corresponding mode shapes are obtained by solving the standard eigenvalue problem. The model is confirmed by comparing the obtained results with benchmark results existing in the literature. Next, a parametric study is carried out to determine the influences of the material gradation, length scale, and stiffness parameters on the vibration properties of multiple functionally graded nanobeams. It is demonstrated that these parameters are vital in examination of the free vibration of a multi-layered FG nanobeam.

1 Introduction

Of the superior mechanical, thermal, and electrical characteristics of micro/nanostructures, the applications in small-scale systems, such as micro-sensors, micro-actuators, and micro-resonators have raised increasingly over the past decade. In order to accurately design these devices and to increase the reliability of the nanostructures, comprehensive study and precise evaluation of the mechanical behaviors of nanostructures, such as bending, buckling, vibration, and wave propagation is crucial. In the literature, to analyze nanostructures, three methods have been used including atomistic modeling (Ball 2001; Baughman et al. 2002), hybrid atomistic–continuum mechanics (Bodily and Sun 2003; Li and Chou 2003), and continuum mechanics.

The two former modeling are computationally costly and can be used only to a few atoms or molecules, thus continuum mechanics is usually used by researchers.

Based on experimental outcomes, it is exposed that small-scale effects play an important role in the static and dynamic properties and responses of micro/nanostructures. Since classical continuum theory is scale-free in modeling material, therefore, size-dependent continuum theories must be applied in order to take into account size effects. Several researchers suggested modified elasticity theories to extract the most accurate results, for example strain gradient elasticity, couple stress, Eringen's nonlocal elasticity, and general nonlocal elasticity (Eringen 2002; Yang et al. 2002; Lam et al. 2003; Shaat and Abdelkefi 2017). Among these non-classical continuum theories, Eringen nonlocal elasticity is more popular in the research community. Eringen (1983, 2006) proposed integral and differential types of constitutive equations with a single material parameter, such that it takes into consideration the forces between atoms and internal length scale. Many researchers have studied the mechanical behaviors of different types of nanostructures within the framework of nonlocal continuum mechanics.

✉ A. Abdelkefi
abdu@nmsu.edu

¹ Faculty of Mechanical Engineering, Urmia University of Technology, Urmia, Iran

² Mechanical and Maintenance Engineering Department, German Jordanian University, Amman 11180, Jordan

³ Department of Mechanical and Aerospace Engineering, New Mexico State University, Las Cruces, NM 88003, USA

Micro/nanobeams are one of the significant elements of most micro/nanostructures, the following literature review focuses on examinations on the vibrational properties of single micro/nanobeams using nonlocal elasticity theories. Roque et al. (2011) employed Eringen's nonlocal theory to reveal the bending, buckling, and vibrational properties of a nanobeam via Timoshenko beam theory. They applied an effective meshless method to obtain their results. Murmu and Pradhan (2009) investigated the vibration response of non-uniform cantilever beam utilizing the nonlocal elasticity theory. Differential quadrature method has been employed and natural frequencies of the structure were determined. They demonstrated that the nonlocal frequency solutions of nano-cantilever are larger compared to the local solutions till a critical height ratio. Thai (2012) studied the analysis of the bending, buckling, and vibration of a nanobeam based on Eringen's theory and a shear deformation beam model. Their model is similar the nonlocal Euler–Bernoulli beam model and does not need a shear correction factor. Aranda-Ruiz et al. (2012) examined the free vibration of a rotating non-uniform nanocantilever by employing Eringen's nonlocal theory. They measured the influence of the small-scale nonlocal phenomenon and angular speed on the vibrational behaviors of nanobeams.

Reddy (2007, 2010), Reddy and El-Borgi (2014) suggested new equations of motion for Euler–Bernoulli, Timoshenko, and Reddy and Levinson beam theories corresponding on the Eringen's nonlocal elasticity theory and then developed analytical solutions for bending, vibrations, and buckling responses of beams for simply supported boundary conditions. Ghadiri and Shafiei (2016) studied the nonlinear bending vibration of nonlocal Euler–Bernoulli nanobeams with considering von Karman nonlinearity and axial loads. The differential quadrature method in combination with a direct iterative approach is implemented to achieve the nonlinear vibration frequencies of nanobeam. Wang et al. (2007) used the Hamilton's principle, Eringen's nonlocal elasticity theory, and Timoshenko beam theory to study the free vibration problem of micro/nano-beams. The governing equations were analytically solved for the natural frequencies of beams with various boundary conditions. Khaniki (2018a, b) applied mixed local/nonlocal Eringen elasticity to examine the transverse vibration properties of a rotating Euler–Bernoulli cantilever beam with considering in-phase and out-of-phase vibrations. Several other studies used nonlocal elasticity theories to model various kinds of dynamical systems.

All aforementioned works considered single micro/nanostructure-based systems for static and dynamic analyses. More complex nanoscale systems contain of two and more prepared nanostructures, such as tubes, rods,

beams, and plates, which are generally joined through some mediums. The static and dynamic properties of such systems are still not fully discovered in the literature. The simplest model of a coupled multiple-nanostructure systems is double nanostructure-based system. It can be composed of two nanotubes, nanorods, nanobeams, or nanoplates. These multiple systems are coupled through a medium with elastic or viscoelastic behaviors. Liu et al. (2017) applied the nonlocal theory along with the Kelvin model to conduct the flexural vibrations of double-viscoelastic-functionally graded nanoplates resting on a viscoelastic Pasternak medium, and subjected to in-plane loads. They obtained analytical solutions for vibrational frequencies and buckling loads when the system was under simply supported boundary conditions. Murmu and Adhikari (2010a, b, 2011), Murmu et al. (2013) examined a comprehensive vibration analysis of a double-nanorod, nanobeam, and nanoplate systems. They obtained the governing equations of motion based on the D'Alembert's principle and nonlocal elasticity theory. They carried out the impact of small-scale effects and other physical parameters on natural frequencies and critical buckling loads and their obtained analytical results were compared to molecular dynamics simulations. Şimşek (2011) proposed an analytical approach for the forced vibration of an elastically connected double-carbon nanotube system carrying a moving nanoparticle corresponding on the nonlocal elasticity theory. The two nanotubes are uniform and are attached with each other constantly by elastic springs. He showed that the dynamic deflections anticipated by the classical theory are always smaller than those expected by the nonlocal theory due to the nonlocal effects.

Arash and Wang (2011) examined the vibration characteristics of single- and double-layered graphene sheets by using nonlocal continuum theory and molecular dynamics simulations. They showed that the classical elastic model overvalued the resonant frequencies of the sheets. Sari et al. (2020) studied the natural vibration behavior of axially functionally graded double nanobeams based on the Euler–Bernoulli beam and Eringen's nonlocal elasticity theory. They modeled the double nanobeams by a layer of linear springs and used the Hamilton's principle for developing the governing differential equation of motion and the Chebyshev spectral collocation method was used to transform the coupled governing differential equations of motion into algebraic equations. Also, they examined the influence the coupling springs, Winkler stiffness, the shear stiffness parameter, taper ratios, and the boundary conditions on the natural transverse frequencies of axially functionally graded double nanobeams. Hashemi and Khaniki (2018) carried out dynamic response of multiple nanobeam system subjected to a moving nanoparticle. They coupled beam layers by Winkler elastic medium and

the nonlocal Euler–Bernoulli beam theory was employed to model each layer of beam. The Hamilton’s principle, eigenvalue function procedure, and the Laplace transform process were applied to solve the equation of motion. Karličić et al. (2018) investigated the dynamic stability of a nonlinear multiple-nanobeam system within the framework of Eringen’s nonlocal theory. They used the incremental harmonic balance procedure to reveal the dynamic stability problem of a nonlinear multiple-nanobeam system.

Sun et al. (2018) studied the design and fabricated of multi-layer graphene reinforced nanostructured functionally graded cemented carbides. Li et al. (2019) investigated the static bending deformation of multi-layered nanoplate under surface loading by using the modified couple stress theory. Guo et al. (2018) presented a three dimensional size dependent layered model for functionally graded magneto-electroelastic plate by using the modified couple stress theory. They reduced the final governing equations to eigen-system by suggesting the extended displacement according to two dimensional Fourier series. Li et al. (2019) studied the size-dependent thermo-electromechanical responses of multi-layered piezoelectric nanoplates subject to heating load. Chen et al. (2017) presented analytical solutions for propagating of time-harmonic waves in three dimensional isotropic multi-layered plates with nonlocal influence. They showed the effect of the nonlocal parameter, stacking sequence on the time-harmonic field response. Study of the static and dynamic properties of such systems has been an interesting outlook in the last decade because of potential applications in design techniques of different micro/nanoengineering systems, particularly when they are expected to be used in vibrating nanodevices, such as resonators, sensors, or other nano-electromechanical systems.

The lack of consistent dynamic models of multiple-nanostructure-based systems creates a challenging study in this field as an interesting task for researchers. A pivotal idea of this work is to fill this gap in the literature and suggest new model and approach of a solution to examine the vibration of double and multiple functionally graded Timoshenko nanobeams (MFGTB) using the nonlocal elasticity theory. The current model of MFGTB composed of multiple individual simply supported and clamped Timoshenko nanobeams that are parallel to each other and joined by an elastic layer of continuous linear springs. The governing equations of motion are derived and the Chebyshev spectral collocation method (CSCM) is applied to find the dimensionless natural frequencies and the corresponding mode shapes.

2 General formulation for FGM nanobeam resting on an elastic foundation

In Fig. 1, a functionally graded multi-layered nanobeam of length L , width b , and thickness h is shown. These nanobeams are connected by a set of linear elastic springs. Based on Timoshenko beam model and considering the double nanobeams scenario, the axial displacement u_x , and the transverse displacement u_z of any point of the beam are given as:

$$u_{ix}(x, z, t) = u_i(x, t) + z\theta_i(x, t), \tag{1}$$

$$u_{iz}(x, z, t) = w_i(x, t), \tag{2}$$

where u_i and w_i ($i = 1, 2$) are the axial and the transverse displacements of any point on the neutral axis of beam i , and θ_i is the bending rotation of the cross-sections at any point on the neutral axis of beam i , x and z are the coordinates along the length and the thickness of the beam, respectively, and t is the time.

The nonzero strain of the beam can be expressed as:

$$\varepsilon_{ixx} = \left(\frac{\partial u_i}{\partial x} + z \frac{\partial \theta_i}{\partial x} \right), \tag{3}$$

$$\gamma_{izx} = \frac{\partial w_i}{\partial x} + \theta_i, \tag{4}$$

where ε_{xx} and γ_{zx} are the normal and shear strains, respectively.

Consider the Hamilton’s principle which is given as:

$$\int_0^t \delta(T_i - U_i - V_i)dt = 0, \tag{5}$$

where δ is the variation operator, T represents the kinetic energy, U is the strain energy, and V denotes the potential energy due to the coupling spring.

Following the strategy used in (Rahmani and Pedram 2014) for one single beam, the first variation of the strain energy and the potential energy for double connected beams can be expressed as:

$$\delta U_i = \int_0^L \left(N_i \left(\frac{\partial \delta u_i}{\partial x} \right) + M_i \left(\frac{\partial \delta \theta_i}{\partial x} \right) + Q_i \left(\frac{\partial \delta w_i}{\partial x} + \delta \theta_i \right) \right) dx, \tag{6}$$

$$\delta V = \int_0^L K(w_2 - w_1)\delta(w_2 - w_1)dx, \tag{7}$$

where N is the axial normal force, Q represents the shear force, M is the bending moment, and K is the stiffness of the elastic layer. These stress resultants are defined as:

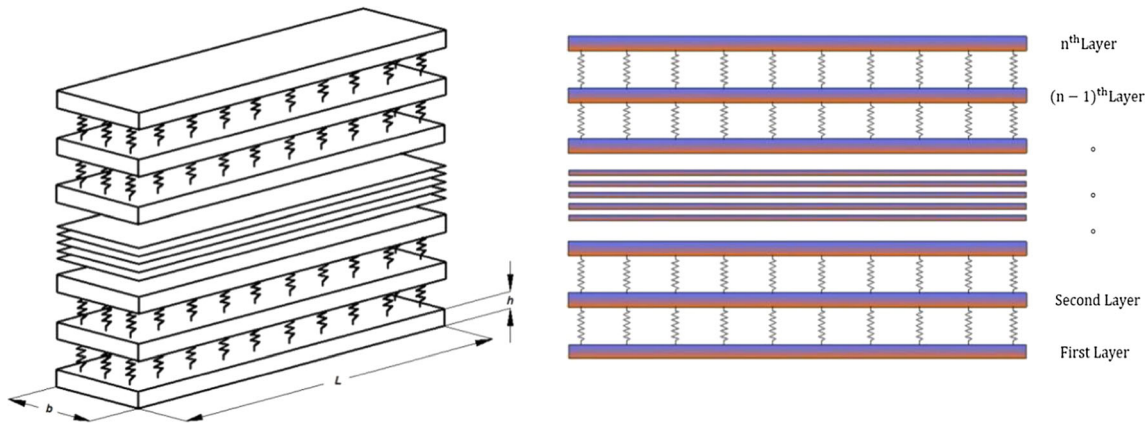


Fig. 1 Schematic illustration of multi-layered nanobeam

$$N = \int_A \sigma_{xx} dA, M = \int_A z \sigma_{xx} dA, Q = \int_A \kappa \sigma_{xz} dA, \tag{8}$$

where σ_{xx} and σ_{xz} are the normal and shear stresses, respectively, A denotes the beam’s cross sectional area which is given as $A = bh$, and κ is the shear correction factor.

The first variation of the kinetic energy of the beam can be given as:

$$\delta T_i = \int_0^L (I_0 \dot{u}_i \delta \dot{u}_i + I_1 \dot{u}_i \delta \dot{\theta}_i + I_1 \dot{\theta}_i \delta \dot{u}_i + I_2 \dot{\theta}_i \delta \dot{\theta}_i + I_0 \dot{w}_i \delta \dot{w}_i) dx, \tag{9}$$

where

$$\{I_0, I_1, I_2\} = \int_A \rho(z) \{1, z, z^2\} dA, \tag{10}$$

and $\rho(z)$ is the density of the beam’s material. Inserting Eqs. (6), (7), and (9) into Eq. (5) yields:

$$\int_0^t \int_0^L \left(N_i \left(\frac{\partial \delta u_i}{\partial x} \right) + M_i \left(\frac{\partial \delta \theta_i}{\partial x} \right) + Q_i \left(\frac{\partial \delta w_i}{\partial x} + \delta \theta_i \right) - K(w_2 - w_1) \delta(w_2 - w_1) \right) dx - \int_0^L (I_0 \dot{u}_i \delta \dot{u}_i + I_1 \dot{u}_i \delta \dot{\theta}_i + I_1 \dot{\theta}_i \delta \dot{u}_i + I_2 \dot{\theta}_i \delta \dot{\theta}_i + I_0 \dot{w}_i \delta \dot{w}_i) dx = 0. \tag{11}$$

Integrating by parts yields:

$$\int_0^t \int_0^L \left\{ \left(\frac{\partial N_i}{\partial x} - I_0 \ddot{u}_i - I_1 \ddot{\theta}_i \right) \delta u_i + \left(\frac{\partial M_i}{\partial x} - Q_i - I_1 \ddot{u}_i - I_2 \ddot{\theta}_i \right) \delta \theta_i + \left(\frac{\partial Q_i}{\partial x} - I_0 \ddot{w}_i - K(w_2 - w_1) \right) \delta(w_2 - w_1) \right\} dx dt + \int_0^L \{ (I_0 \dot{u}_i + I_1 \dot{\theta}_i) \delta \dot{u}_i + (I_1 \dot{u}_i + I_2 \dot{\theta}_i) \delta \dot{\theta}_i + I_0 \dot{w}_i \delta \dot{w}_i \} dx - \int_0^t \{ N_i \delta u_i + M_i \delta \theta_i + Q_i \delta w_i \}_0^L dt = 0 \tag{12}$$

According to the Hamilton’s principle, the equations of motion can be written as:

$$\frac{\partial N_i}{\partial x} - I_0 \ddot{u}_i - I_1 \ddot{\theta}_i = 0, \tag{13}$$

$$\frac{\partial M_i}{\partial x} - Q_i - I_1 \ddot{u}_i - I_2 \ddot{\theta}_i = 0, \tag{14}$$

$$\frac{\partial Q_i}{\partial x} - I_0 \ddot{w}_i + (-1)^i K(w_1 - w_2) = 0. \tag{15}$$

The boundary conditions that are related to Eq. (12) can be expressed as follows:

$$N_i = 0 \text{ or } u_i = 0 \text{ at } x = 0 \text{ and } x = L, \tag{16}$$

$$M_i = 0 \text{ or } \theta_i = 0 \text{ at } x = 0 \text{ and } x = L, \tag{17}$$

$$Q_i = 0 \text{ or } w_i = 0 \text{ at } x = 0 \text{ and } x = L. \tag{18}$$

3 Nonlocal Timoshenko modeling of multi-layers FG nanobeams

Based on Eringen’s nonlocal elasticity theory, the stress at a reference point in a structure is a function of the strains at all points in the domain. For nonlocal FG Timoshenko

beam, the nonlocal constitutive relations may be written as follows (Sari et al. 2020):

$$\sigma_{ixx} - (e_0a)^2 \frac{\partial^2 \sigma_{ixx}}{\partial x^2} = E(z)\epsilon_{ixx}, \tag{19}$$

$$\tau_{izx} - (e_0a)^2 \frac{\partial^2 \tau_{izx}}{\partial x^2} = G(z)\gamma_{izx}, \tag{20}$$

where e_0 is a constant that depends on the material properties, a represents the internal characteristic length, $E(z)$ is the modulus of elasticity, and $G(z) = E(z)/[2(1 + \nu)]$ is the shear modulus.

By using Eqs. (3), (4), (8), (19), and (20) and following the strategy used in (Rahmani and Pedram 2014), the axial force, bending moment, and shear force of the nonlocal Timoshenko beam are expressed as:

$$N_i - \eta^2 \frac{\partial^2 N_i}{\partial x^2} = S_0 \frac{\partial u_i}{\partial x} + S_1 \frac{\partial \theta_i}{\partial x}, \tag{21}$$

$$M_i - \eta^2 \frac{\partial^2 M_i}{\partial x^2} = S_1 \frac{\partial u_i}{\partial x} + S_2 \frac{\partial \theta_i}{\partial x}, \tag{22}$$

$$Q_i - \eta^2 \frac{\partial^2 Q_i}{\partial x^2} = S_3 \left(\frac{\partial w_i}{\partial x} + \theta_i \right), \tag{23}$$

where

$$(S_0, S_1, S_2) = \int_A E(z)(1, z, z^2) dA, \tag{24}$$

$$S_3 = \int_A \kappa G(z) dA, \tag{25}$$

and $\eta = e_0a$.

In this study, $E(z)$, $G(z)$, and $\rho(z)$ are given as (Rahmani and Pedram 2014):

$$E(z) = (E_c - E_m) \left(\frac{z}{h} + \frac{1}{2} \right)^k + E_m, \tag{26}$$

$$G(z) = (G_c - G_m) \left(\frac{z}{h} + \frac{1}{2} \right)^k + G_m, \tag{27}$$

$$\rho(z) = (\rho_c - \rho_m) \left(\frac{z}{h} + \frac{1}{2} \right)^k + \rho_m, \tag{28}$$

where the subscripts m and c represent the metallic and ceramic rich surfaces. The top surface ($z = h/2$) of the beam is ceramic-rich whereas the bottom surface ($z = -h/2$) is metal-rich, and k is the radiant index that is considered to describe the change in the volume fraction of the constituent materials of the FG beam.

By using Eqs. (13)–(15) and (21)–(23), the equations of motion of two FG Timoshenko nanobeams connected by a continuous layer of vertical translational springs are given as:

$$S_0 \frac{\partial^2 u_1}{\partial x^2} + S_1 \frac{\partial^2 \theta_1}{\partial x^2} = I_0 \frac{\partial^2 u_1}{\partial t^2} + I_1 \frac{\partial^2 \theta_1}{\partial t^2} - \eta^2 \left(I_0 \frac{\partial^4 u_1}{\partial x^2 \partial t^2} + I_1 \frac{\partial^4 \theta_1}{\partial x^2 \partial t^2} \right), \tag{29}$$

$$S_3 \left(\frac{\partial^2 w_1}{\partial x^2} + \frac{\partial \theta_1}{\partial x} \right) - K(w_1 - w_2) + K\eta^2 \left(\frac{\partial^2 w_1}{\partial x^2} - \frac{\partial^2 w_2}{\partial x^2} \right) = I_0 \frac{\partial^2 w_1}{\partial t^2} - \eta^2 I_0 \frac{\partial^4 w_1}{\partial x^2 \partial t^2}, \tag{30}$$

$$S_1 \frac{\partial^2 u_1}{\partial x^2} + S_2 \frac{\partial^2 \theta_1}{\partial x^2} - S_3 \left(\frac{\partial w_1}{\partial x} + \theta_1 \right) = I_1 \frac{\partial^2 u_1}{\partial t^2} + I_2 \frac{\partial^2 \theta_1}{\partial t^2} - \eta^2 \left(I_1 \frac{\partial^4 u_1}{\partial x^2 \partial t^2} + I_2 \frac{\partial^4 \theta_1}{\partial x^2 \partial t^2} \right), \tag{31}$$

$$S_0 \frac{\partial^2 u_2}{\partial x^2} + S_1 \frac{\partial^2 \theta_2}{\partial x^2} = I_0 \frac{\partial^2 u_2}{\partial t^2} + I_1 \frac{\partial^2 \theta_2}{\partial t^2} - \eta^2 \left(I_0 \frac{\partial^4 u_2}{\partial x^2 \partial t^2} + I_1 \frac{\partial^4 \theta_2}{\partial x^2 \partial t^2} \right), \tag{32}$$

$$S_3 \left(\frac{\partial^2 w_2}{\partial x^2} + \frac{\partial \theta_2}{\partial x} \right) - K(w_2 - w_1) + K\eta^2 \left(\frac{\partial^2 w_2}{\partial x^2} - \frac{\partial^2 w_1}{\partial x^2} \right) = I_0 \frac{\partial^2 w_2}{\partial t^2} - \eta^2 I_0 \frac{\partial^4 w_2}{\partial x^2 \partial t^2}, \tag{33}$$

$$S_1 \frac{\partial^2 u_2}{\partial x^2} + S_2 \frac{\partial^2 \theta_2}{\partial x^2} - S_3 \left(\frac{\partial w_2}{\partial x} + \theta_2 \right) = I_1 \frac{\partial^2 u_2}{\partial t^2} + I_2 \frac{\partial^2 \theta_2}{\partial t^2} - \eta^2 \left(I_1 \frac{\partial^4 u_2}{\partial x^2 \partial t^2} + I_2 \frac{\partial^4 \theta_2}{\partial x^2 \partial t^2} \right). \tag{34}$$

An eigenvalue problem analysis is performed by assuming harmonic solutions in time as:

$$(u_i(x, t), w_i(x, t), \theta_i(x, t)) = (U_i(x), W_i(x), \Theta_i(x))e^{j\omega t}, \tag{35}$$

where ω is the natural frequency in rad/s, and $j = \sqrt{-1}$ and U , W , and Θ are as the mode shapes of the system.

Substituting Eq. (35) into Eqs. (29–34) yields:

$$S_0 \frac{d^2 U_1}{dx^2} + S_1 \frac{d^2 \Theta_1}{dx^2} = -\omega^2 I_0 U_1 - \omega^2 I_1 \Theta_1 + \eta^2 \omega^2 \left(I_0 \frac{d^2 U_1}{dx^2} + I_1 \frac{d^2 \Theta_1}{dx^2} \right), \tag{36}$$

$$S_3 \left(\frac{d^2 W_1}{dx^2} + \frac{d\Theta_1}{dx} \right) - K(W_1 - W_2) + K\eta^2 \left(\frac{d^2 W_1}{dx^2} - \frac{d^2 W_2}{dx^2} \right) = -\omega^2 I_0 W_1 + \eta^2 \omega^2 I_0 \frac{d^2 W_1}{dx^2}, \tag{37}$$

$$S_1 \frac{d^2 U_1}{dx^2} + S_2 \frac{d^2 \Theta_1}{dx^2} - S_3 \left(\frac{dW_1}{dx} + \Theta_1 \right) = -\omega^2 I_1 U_1 - \omega^2 I_2 \Theta_1 + \eta^2 \omega^2 \left(I_1 \frac{d^2 U_1}{dx^2} + I_2 \frac{d^2 \Theta_1}{dx^2} \right), \quad (38)$$

$$S_0 \frac{d^2 U_2}{dx^2} + S_1 \frac{d^2 \Theta_2}{dx^2} = -\omega^2 I_0 U_2 - \omega^2 I_1 \Theta_2 + \eta^2 \omega^2 \left(I_0 \frac{d^2 U_2}{dx^2} + I_1 \frac{d^2 \Theta_2}{dx^2} \right), \quad (39)$$

$$S_3 \left(\frac{d^2 W_2}{dx^2} + \frac{d\Theta_2}{dx} \right) - K(W_2 - W_1) + K\eta^2 \left(\frac{d^2 W_2}{dx^2} - \frac{d^2 W_1}{dx^2} \right) = -\omega^2 I_0 W_2 + \eta^2 \omega^2 I_0 \frac{d^2 W_2}{dx^2}, \quad (40)$$

$$S_1 \frac{d^2 U_2}{dx^2} + S_2 \frac{d^2 \Theta_2}{dx^2} - S_3 \left(\frac{dW_2}{dx} + \Theta_2 \right) = -\omega^2 I_1 U_2 - \omega^2 I_2 \Theta_2 + \eta^2 \omega^2 \left(I_1 \frac{d^2 U_2}{dx^2} + I_2 \frac{d^2 \Theta_2}{dx^2} \right). \quad (41)$$

Performing a similar process for multi-layered beams, the governing equation of motions can be expressed in terms of displacements as:

$$S_0 \frac{d^2 U_1}{dx^2} + S_1 \frac{d^2 \Theta_1}{dx^2} = -\omega^2 I_0 U_1 - \omega^2 I_1 \Theta_1 + \eta^2 \omega^2 \left(I_0 \frac{d^2 U_1}{dx^2} + I_1 \frac{d^2 \Theta_1}{dx^2} \right), \quad (42)$$

$$S_3 \left(\frac{d^2 W_1}{dx^2} + \frac{d\Theta_1}{dx} \right) - K_1(W_1 - W_2) + K_1\eta^2 \left(\frac{d^2 W_1}{dx^2} - \frac{d^2 W_2}{dx^2} \right) = -\omega^2 I_0 W_1 + \eta^2 \omega^2 I_0 \frac{d^2 W_1}{dx^2}, \quad (43)$$

$$S_1 \frac{d^2 U_1}{dx^2} + S_2 \frac{d^2 \Theta_1}{dx^2} - S_3 \left(\frac{dW_1}{dx} + \Theta_1 \right) = -\omega^2 I_1 U_1 - \omega^2 I_2 \Theta_1 + \eta^2 \omega^2 \left(I_1 \frac{d^2 U_1}{dx^2} + I_2 \frac{d^2 \Theta_1}{dx^2} \right), \quad (44)$$

$$S_0 \frac{d^2 U_i}{dx^2} + S_1 \frac{d^2 \Theta_i}{dx^2} = -\omega^2 I_0 U_i - \omega^2 I_1 \Theta_i + \eta^2 \omega^2 \left(I_0 \frac{d^2 U_i}{dx^2} + I_1 \frac{d^2 \Theta_i}{dx^2} \right), \quad (45)$$

$$S_3 \left(\frac{d^2 W_i}{dx^2} + \frac{d\Theta_i}{dx} \right) - K_{i-1}(W_i - W_{i-1}) + K_{i-1}\eta^2 \left(\frac{d^2 W_i}{dx^2} - \frac{d^2 W_{i-1}}{dx^2} \right) - K_i(W_i - W_{i+1}) + K_i\eta^2 \left(\frac{d^2 W_i}{dx^2} - \frac{d^2 W_{i+1}}{dx^2} \right) = -\omega^2 I_0 W_i + \eta^2 \omega^2 I_0 \frac{d^2 W_i}{dx^2}, \quad (46)$$

$$S_1 \frac{d^2 U_i}{dx^2} + S_2 \frac{d^2 \Theta_i}{dx^2} - S_3 \left(\frac{dW_i}{dx} + \Theta_i \right) = -\omega^2 I_1 U_i - \omega^2 I_2 \Theta_i + \eta^2 \omega^2 \left(I_1 \frac{d^2 U_i}{dx^2} + I_2 \frac{d^2 \Theta_i}{dx^2} \right). \quad (47)$$

$i = 2, 3, \dots, m-1$

$$S_0 \frac{d^2 U_m}{dx^2} + S_1 \frac{d^2 \Theta_m}{dx^2} = -\omega^2 I_0 U_m - \omega^2 I_1 \Theta_m + \eta^2 \omega^2 \left(I_0 \frac{d^2 U_m}{dx^2} + I_1 \frac{d^2 \Theta_m}{dx^2} \right), \quad (48)$$

$$S_3 \left(\frac{d^2 W_m}{dx^2} + \frac{d\Theta_m}{dx} \right) - K_{m-1}(W_m - W_{m-1}) + K_{m-1}\eta^2 \left(\frac{d^2 W_m}{dx^2} - \frac{d^2 W_{m-1}}{dx^2} \right) = -\omega^2 I_0 W_m + \eta^2 \omega^2 I_0 \frac{d^2 W_m}{dx^2}, \quad (49)$$

$$S_1 \frac{d^2 U_m}{dx^2} + S_2 \frac{d^2 \Theta_m}{dx^2} - S_3 \left(\frac{dW_m}{dx} + \Theta_m \right) = -\omega^2 I_1 U_m - \omega^2 I_2 \Theta_m + \eta^2 \omega^2 \left(I_1 \frac{d^2 U_m}{dx^2} + I_2 \frac{d^2 \Theta_m}{dx^2} \right). \quad (50)$$

It should be mentioned that in the current study the values of the properties for the metallic and the ceramic layers used in the nonlocal FG nanobeams are given in Table 1.

Table 1 Material properties used in the FG beam (Rahmani and Pedram 2014)

Properties	Steel	Alumina (Al ₂ O ₃)
E (GPa)	210	390
ρ (kg/m ³)	7800	3960
ν	0.3	0.24

4 Solution procedure: Chebyshev spectral collocation method (CSCM)

When investigating the vibrations of double and multiple FG Timoshenko nanobeams with different boundary conditions, obtaining analytical solutions becomes challenging. It should be mentioned that the single FG beam case was performed by Rahmani and Pedman (2014) for simply supported boundary conditions in which Fourier series were applied for only one kind of boundary conditions. In this work, different kinds of boundary conditions for single, double, and multiple FG nanobeams are considered and analyzed by using the Chebyshev spectral collocation method. This method is utilized to discretize the equations of motion and obtain the natural frequencies and mode shapes of the system under investigation.

The Chebyshev points are defined in the range of $[-1, 1]$ as (Trefethen 2000):

$$x_j = \cos\left(\frac{j\pi}{N}\right), \quad j = 0, 1, \dots, N. \tag{51}$$

The Chebyshev differentiation matrix, $[D]_N$, is an $(N + 1) \times (N + 1)$ matrix, and its elements are expressed as:

$$\begin{aligned} (D_N)_{00} &= \frac{2N^2 + 1}{6}, \quad (D_N)_{NN} = -\frac{2N^2 + 1}{6}, \\ (D_N)_{jj} &= \frac{-x_j}{2(1 - x_j^2)}, \quad j = 1, \dots, N - 1 \\ (D_N)_{ij} &= \frac{c_i (-1)^{i+j}}{c_j (x_i - x_j)}, \quad i \neq j, \quad i, j = 0, \dots, N, \quad c_i \\ &= \begin{cases} 2, & i = 0 \text{ or } N, \\ 1, & \text{otherwise} \end{cases} \end{aligned} \tag{52}$$

In the current research, the x -axis is normalized to be in the range of $[0, 1]$, hence, the elements of D_N will have different values than those shown in Eq. (51). Due to its accuracy, rapid convergence rate, flexibility and simplicity in utilization, the CSCM has efficiently been applied to investigate the natural vibrations and buckling responses of different structures (Sari et al. 2017; Ma’en et al. 2018; Sari and Butcher 2011). When employing the CSCM to discretize differential equations, the n th derivative of an unknown function (the transverse and axial displacements of the beams, and the bending rotation of the beams) is given by $D_n = (D_N)^n$.

For the FG Timoshenko nonlocal double nanobeam under consideration, each point possesses three degrees of freedom: U , W , and Θ . Hence, a displacement vector is defined as:

$$\{U\} = \left\{ \begin{matrix} U_{1,1}W_{1,1}\Theta_{1,1}U_{2,1}W_{2,1}\Theta_{2,1}U_{1,N+1}W_{1,N+1}\Theta_{1,N+1}U_{2,N+1}W_{2,N+1}\Theta_{2,N+1} \\ U_{1,2}\dots U_{1,N}W_{1,2}\dots W_{1,N}\Theta_{1,2}\dots\Theta_{1,N}U_{2,2}\dots U_{2,N}W_{2,2}\dots W_{2,N}\Theta_{2,2}\dots\Theta_{2,N} \end{matrix} \right\}^T, \tag{53}$$

where the first and second subscripts refer to the i th beam (beam 1 or beam 2), and to the j th Chebyshev point along the beam’s span ($j = 1, 2, \dots, N + 1$), respectively.

The Eqs. (42–50) are discretized using the CSCM as:

$$\begin{bmatrix} GE1 \\ GE2 \\ GE3 \end{bmatrix} \{U\} = \omega^2 \begin{bmatrix} RH1 \\ RH2 \\ RH3 \end{bmatrix} \{U\}, \tag{54}$$

where

$$GE1 = (S_0 * [100000] \otimes D2) + (S_1 * [001000] \otimes D2), \tag{55}$$

$$\begin{aligned} GE2 &= (S_3 * [010000] \otimes D2) + (S_3 * [001000] \otimes D1) \\ &\quad - (K * [010000] \otimes I) + (K * [000010] \otimes D1) \\ &\quad + (K\eta^2 * [010000] \otimes D2) \\ &\quad - (K\eta^2 * [000010] \otimes D2), \end{aligned} \tag{56}$$

$$\begin{aligned} GE3 &= (S_1 * [100000] \otimes D2) + (S_2 * [001000] \otimes D2) \\ &\quad - (S_3 * [010000] \otimes D1) - (S_3 * [001000] \otimes I), \end{aligned} \tag{57}$$

$$GE4 = (S_0 * [000100] \otimes D2) + (S_1 * [000001] \otimes D2), \tag{58}$$

$$\begin{aligned} GE5 &= (S_3 * [000010] \otimes D2) + (S_3 * [000001] \otimes D1) \\ &\quad - (K * [000010] \otimes I) + (K * [010000] \otimes D1) \\ &\quad + (K\eta^2 * [000010] \otimes D2) \\ &\quad - (K\eta^2 * [010000] \otimes D2), \end{aligned} \tag{59}$$

$$\begin{aligned} GE6 &= (S_1 * [000100] \otimes D2) + (S_2 * [000001] \otimes D2) \\ &\quad - (S_3 * [000010] \otimes D1) - (S_3 * [000001] \otimes I), \end{aligned} \tag{60}$$

$$\begin{aligned} RH1 &= (-I_0 * [100000] \otimes I) - (I_1 * [001000] \otimes I) \\ &\quad + (I_0\eta^2 * [100000] \otimes D2) \\ &\quad + (I_1\eta^2 * [001000] \otimes D2), \end{aligned} \tag{61}$$

$$RH2 = (-I_0 * [010000] \otimes I) + (I_0\eta^2 * [010000] \otimes D2), \tag{62}$$

$$\begin{aligned} RH3 &= (-I_1 * [100000] \otimes I) - (I_2 * [001000] \otimes I) \\ &\quad + (I_1\eta^2 * [100000] \otimes D2) \\ &\quad + (I_2\eta^2 * [001000] \otimes D2), \end{aligned} \tag{63}$$

$$RH4 = (-I_0 * [000100] \otimes I) - (I_1 * [000001] \otimes I) + (I_0 \eta^2 * [000100] \otimes D2) + (I_1 \eta^2 * [000001] \otimes D2), \tag{64}$$

$$RH5 = (-I_0 * [000010] \otimes I) + (I_0 \eta^2 * [000010] \otimes D2), \tag{65}$$

$$RH6 = (-I_1 * [000100] \otimes I) - (I_2 * [000001] \otimes I) + (I_1 \eta^2 * [000100] \otimes D2) + (I_2 \eta^2 * [000001] \otimes D2), \tag{66}$$

and \otimes is the Kronecker product.

The size of each term (*GE1*, *GE2*, ..., *GE6*, *RH1*, *RH2*, ..., and *RH6*) is $(N + 1) \times 6(N + 1)$. The same scheme is followed for the triple nonlocal FG Timoshenko nanobeams. After rewriting the equations of motion according to the CSCM, the eigenvalue problem for the FG Timoshenko double nanobeams with clamped (C) and simply supported (S) boundary conditions can be solved. More details can be found in (Sari and Butcher 2011).

Table 2 Fundamental nondimensional natural frequency $\hat{\omega}_1 = \omega_1 L^2 \sqrt{\rho_c A / E_c I}$ of simply supported nanobeams ($b = 1000 \times 10^{-9} m$, $L = 10000 \times 10^{-9} m$, $k = 10$, $\kappa = 5/6$)

L/h	$(e_0 a)^2$	Rahmani and Pedram (2014)	Present
20	0	5.6521	5.6528
	1×10^{-12}	5.3923	5.3929
	2×10^{-12}	5.1653	5.1659
	3×10^{-12}	4.9647	4.9653
	4×10^{-12}	4.7858	4.7864
50	5×10^{-12}	4.6250	4.6255
	0×10^{-12}	5.6730	5.6736
	1×10^{-12}	5.4122	5.4128
	2×10^{-12}	5.1843	5.1849
	3×10^{-12}	4.9830	4.9836
100	4×10^{-12}	4.8035	4.8040
	5×10^{-12}	4.6421	4.6426
	0×10^{-12}	5.6760	5.6766
	1×10^{-12}	5.4150	5.4156
	2×10^{-12}	5.1871	5.1877
	3×10^{-12}	4.9857	4.9862
	4×10^{-12}	4.8060	4.8066
	5×10^{-12}	4.6445	4.6450

5 Results and discussions

5.1 Methodology verification for single nonlocal Timoshenko FG beams

In order to check the accuracy of the CSCM, a comparative study is first performed. Initially, the natural frequencies of the FG Timoshenko nonlocal single nanobeam are compared to those reported by Rahmani and Pedram (Rahmani and Pedram 2014). In Table 2, the nondimensional fundamental frequencies of simply supported FG Timoshenko nanobeams are shown which are defined as $\hat{\omega}_1 = \omega_1 L^2 \sqrt{\rho_c A / E_c I}$. Also, Table 3 presents the nondimensional fundamental frequencies of simply supported FG Timoshenko nanobeams for two different the power-law exponent, namely, $k = 1$ and $k = 5$. It follows from the obtained results in these tables that the natural frequencies of the present methodology are in acceptable agreement with those calculated by Rahmani and Pedram (2014). Tables 2 and 3 reflects the reliability of the numerical technique used in this study.

The plotted curves in Fig. 2 show the variations of the first fundamental natural frequency when the material gradation distribution is varied and the nonlocal parameter is set equal to $l/h = 100$. It can be seen that the first natural frequency significantly decreases when the power exponent changes from 0 to 5 than that when power exponent in range between 5 and 10. In addition, an increase in the nonlocal parameter has a softening effect on the natural frequency of the system, as expected. These results are in excellent agreement with their counterparts obtained by Rahmani and Pedram (2014).

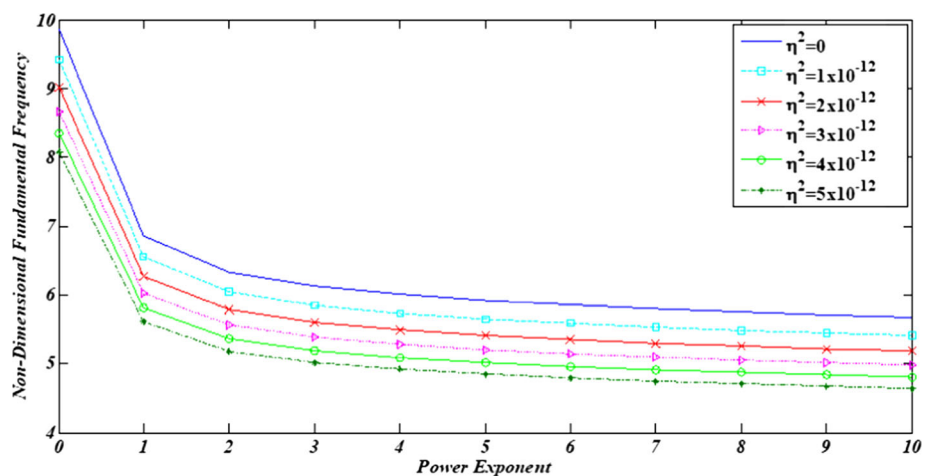
5.2 Vibration properties of double connected FG nanobeams

The effects of the power exponent of the material, nonlocal elasticity, and continuous elastic layer stiffness on the natural frequencies of the double connected FG nanobeams are investigated. The plotted curves in Fig. 3 show the influence of the power exponent parameter (k) at different values of the nonlocal parameter (η^2) on the first three dimensionless natural frequencies of FG SS–SS double nanobeam with considering the stiffness of the continuous elastic layer between the nanobeams equal to $K = 500 N/m$ when $L/h = 20$. The notation SS–SS indicates that the two nanobeams are simply-supported at both edges. The power exponent parameter is considered to be in the interval of $[0, 10]$. Inspecting the plots in Fig. 3, it is clear that both the power exponent parameter and nonlocal elasticity parameter have a softening effect on the first three natural frequencies of the coupled system. This is

Table 3 Fundamental frequency parameter $\Omega_1 = \omega_1 L^2 \sqrt{\rho_c A / E_c I}$ of simply supported nanobeams ($b = 1000 \times 10^{-9} m$, $L = 10,000 \times 10^{-9} m$, $\kappa = 5/6$)

L/h	$k = 1.0$			$k = 5.0$		
	$(e_0 a)^2$	Rahmani and Pedram (2014)	Present	Rahmani and Pedram (2014)	Present	
20	0	6.9676	6.8370	5.9172	5.8993	
	1×10^{-12}	6.6473	6.5227	5.6452	5.6281	
	2×10^{-12}	6.3674	6.2481	5.4075	5.3912	
	3×10^{-12}	6.1202	6.0055	5.1975	5.1819	
	4×10^{-12}	5.8997	5.7892	5.0103	4.9952	
50	5×10^{-12}	5.7014	5.5946	4.8419	4.8273	
	0×10^{-12}	6.9917	6.8605	5.9389	5.9209	
	1×10^{-12}	6.6703	6.5451	5.6659	5.6487	
	2×10^{-12}	6.3895	6.2695	5.4274	5.4109	
	3×10^{-12}	6.1414	6.0261	5.2166	5.2008	
100	4×10^{-12}	5.9201	5.8090	5.0287	5.0134	
	5×10^{-12}	5.7212	5.6138	4.8597	4.8450	
	0×10^{-12}	6.9952	6.8638	5.9421	5.9240	
	1×10^{-12}	6.6736	6.5483	5.6689	5.6517	
	2×10^{-12}	6.3927	6.2726	5.4302	5.4138	
	3×10^{-12}	6.1444	6.0291	5.2194	5.2036	
	4×10^{-12}	5.9231	5.8118	5.03135	5.0161	
	5×10^{-12}	5.7240	5.6165	4.8623	4.8475	

Fig. 2 Variation of the first natural frequency of a simply supported single nanobeam with material gradation for different nonlocality parameter at $L/h = 100$



expected because an increase in the power exponent parameter is associated with a decrease in the effective Young’s modulus of the structure and hence a reduction in the natural frequencies of the system. Moreover, this figure shows that the reduction of the natural frequencies is more noticeable for the higher modes when the power exponent parameter is increased. Deeply investigating the influences of the power exponent parameter on the natural frequencies, it can be noted that these frequencies are in general more sensitive when k is in the range of $[0, 2]$ for various configurations of the nonlocal parameter. Furthermore, for higher values of the nonlocal parameter, it is observed that the second and third natural frequencies becomes closer to each other which can result in the

presence of a one-to-one internal resonance. This trend becomes more important when the power exponent is increased.

The plotted curves in Fig. 4 present the impact of the power exponent parameter (k) for different values of the nonlocal parameter (η^2) on the first three dimensionless frequencies of FG CC–CC double nanobeam with $K = 500 N/m$, and $L/h = 20$. The notation CC–CC denotes that the two nanobeams are clamped at both boundaries. As predicted, it follows from these plots that both k and η^2 parameters have softening influence on the first three natural frequencies. Furthermore, this figure reveals that the reduction of the natural frequencies is more significant for the higher modes. Besides, the frequencies

Fig. 3 Variations of the first three natural frequencies with respect to the power exponent parameter for different values of the nonlocal parameter for a FG SS–SS Timoshenko double nanobeam when ($K = 500\text{ N/m}$, $L/h = 20$)

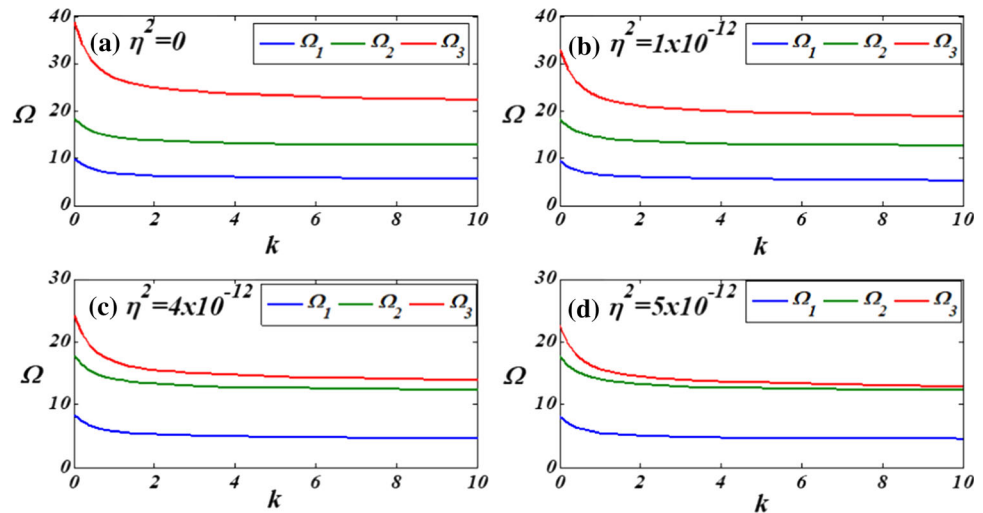
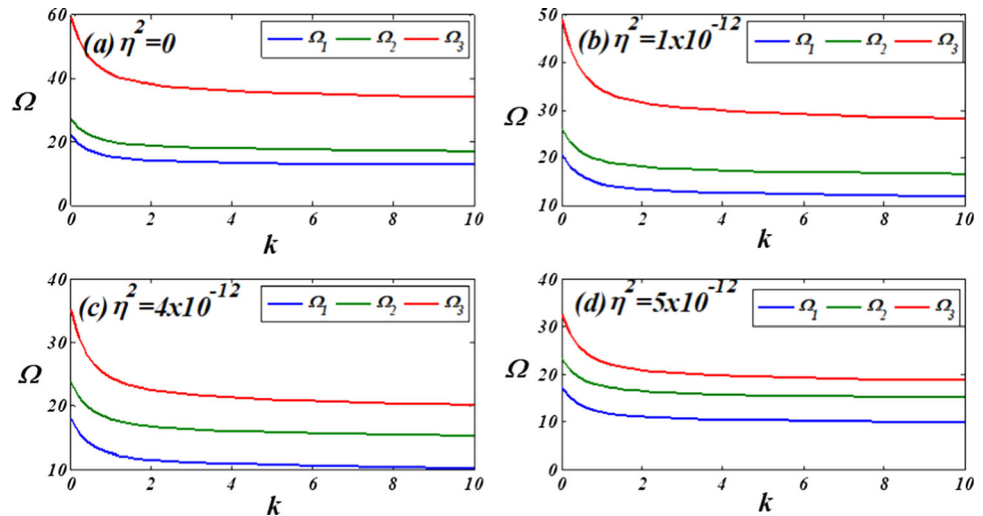


Fig. 4 Variations of the first three natural frequencies with respect to the power exponent parameter for different values of the nonlocal parameter for a FG CC–CC Timoshenko double nanobeam when ($K = 500\text{ N/m}$, $L/h = 20$)



are in general more sensitive when k is in the range of $[0, 4]$. It follows from the plotted curves in Figs. 3 and 4 that the coupling stiffness between the two beams has a less effect on the clamped–clamped configuration compared to the simply supported counterpart. Indeed, the second and third natural frequencies are almost the same for the SS–SS configuration when the nonlocal parameter is $\eta^2 = 5 \times 10^{-12}$, as shown in Fig. 3, however, for the same value of the linear coupling stiffness, these two natural frequencies become far away than each other for the CC–CC configuration, as indicated in Fig. 4.

The effects of the nonlocal elasticity parameter for four distinct values of the power exponent on the first three dimensionless natural frequencies of FG SS–SS and FG CC–CC double nanobeam with $K = 1000\text{ N/m}$ and $L/h = 50$ are presented in Figs. 5 and 6, respectively. It is obvious that both k and η^2 parameters have a softening impact on the natural frequencies of the double beam system. Moreover, these figures reveal that the reduction of the first

mode with respect to the nonlocal parameter is less pronounced compared to the higher modes. It should be mentioned that for both considered boundary conditions, the first three transverse natural frequencies are in general more sensitive for values of the nonlocal parameter in the range of 0 and 3×10^{-12} .

To further investigate the impacts of the linear stiffness coupling between the two connected FG beams on the natural frequencies of the coupled system, Fig. 7 reveals the influence of the stiffness parameter (K) for two values of the power exponent (k) on the first four dimensionless transverse frequencies of FG SS–SS double nanobeam with $\eta^2 = 1 \times 10^{-12}$ and $L/h = 50$. The stiffness parameter is assumed to be in the interval $[0, 1000\text{ (N/m)}]$. It is clear that the alteration of the natural frequencies take place by increasing the linear stiffness coupling parameter. It follows from the plots in Fig. 7 that the first dimensionless transverse frequency is not sensitive to the change in the linear stiffness coupling parameter due to the symmetry of

Fig. 5 Variations of the first three natural frequencies with respect to the nonlocal parameter for different values of the power exponent parameter for a FG SS–SS Timoshenko double nanobeam when ($K = 1000\text{ N/m}$, $L/h = 50$)

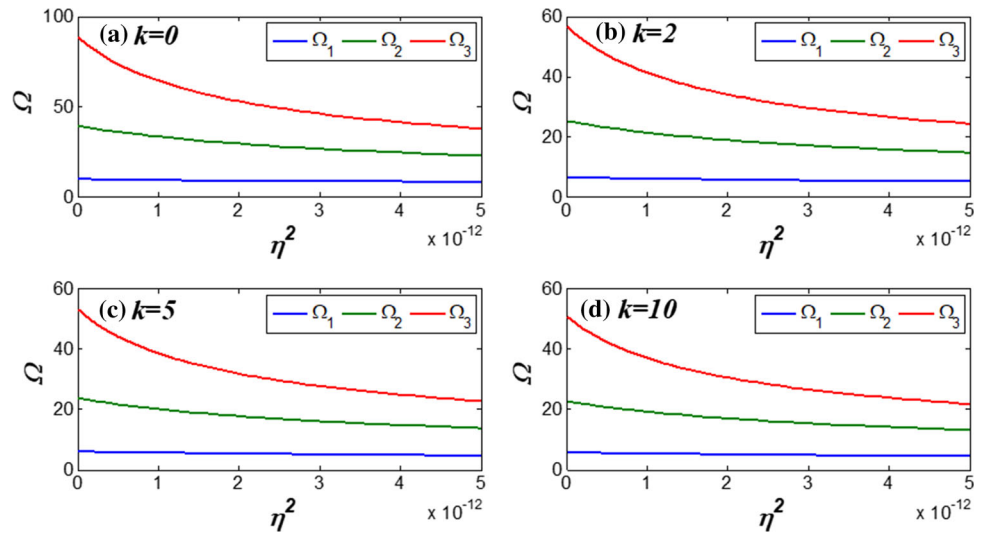


Fig. 6 Variations of the first three natural frequencies with respect to the nonlocal parameter for different values of the power exponent parameter for a FG CC–CC Timoshenko double nanobeam when ($K = 1000\text{ N/m}$, $L/h = 50$)

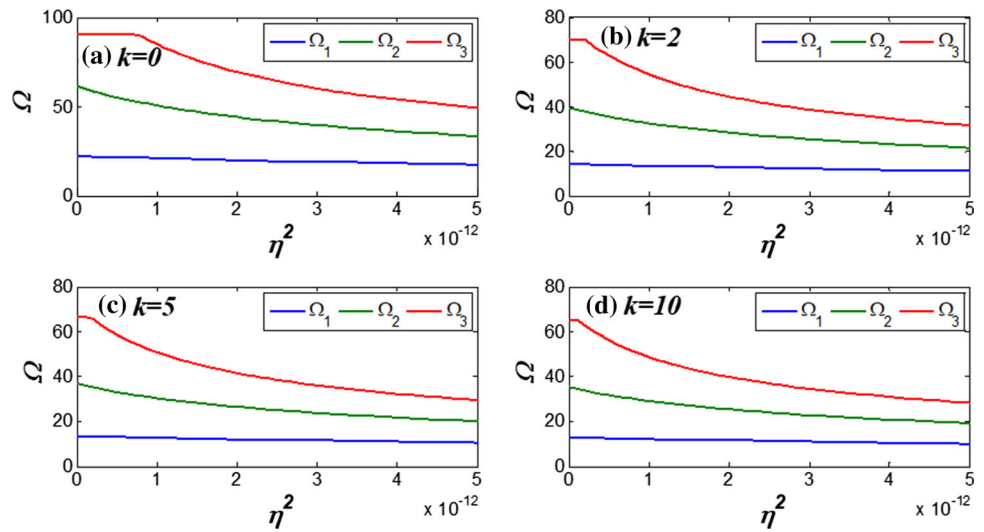
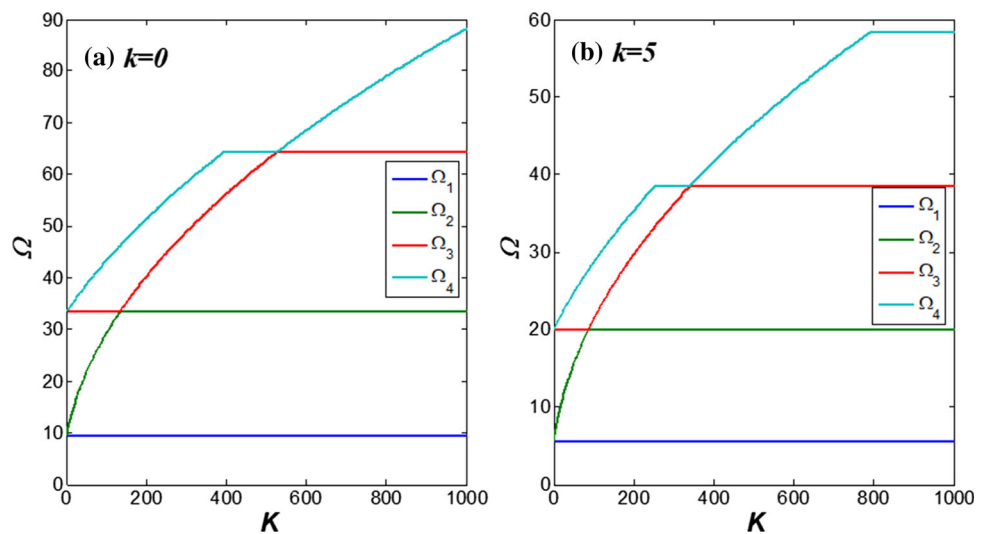


Fig. 7 Variations of Ω_1 , Ω_2 , Ω_3 , and Ω_4 as function of the stiffness parameter at different values of the power exponent for a FG SS–SS Timoshenko double nanobeam ($\eta^2 = 1 \times 10^{-12}$, $L/h = 50$)



the coupled system (the two beams are identical). On the other hand, the second natural frequency is first increased by increasing the stiffness parameter after that it is not sensitive to changing in the stiffness parameter after a crossing phenomenon takes place. For instance, in a fixed power exponent ($k = 5$), the second natural frequency is increased when the linear stiffness coupling parameter is altered from 0 to 88 N/m, while by increasing the stiffness parameter from 88 to 1000 N/m, the second natural frequency is almost unaffected.

The alteration of the third natural frequency has three stages when the linear stiffness coupling parameter is increased, as indicated in Fig. 7. First it is constant, then it is increased and last stage it stabilizes to a constant value. This is due to the crossing between the modes of the two coupled beams. For instance, in a fixed power exponent ($k = 5$), the third natural frequency is unchangeable when the stiffness parameter is altered from zero to 88 N/m, then by increasing the linear stiffness coupling parameter from 88 to 342 N/m, the third natural frequency is increased while it is constant when the stiffness parameter is changed from 342 to 1000 N/m. As depicted in the plotted curves in Fig. 7, the fourth natural frequency has a similar behavior as the third natural frequency by increasing the stiffness parameter. From another perspective, the plotted curves in Fig. 7 can be seen as three constant curves for the first, third, and fifth coupled natural frequencies and two (second and fourth) continuously increasing frequencies with respect to the linear coupled spring. The unchangeable values of the three constant frequencies are due to the identical properties, dimensions, and boundary conditions of the two selected beams.

To examine the effects of the linear coupling stiffness on the mode shapes of the coupled system, the mode shapes of FG SS–SS double nanobeams for two distinct values of

spring (K) before and after the first and second crossing when $k = 0$, $\eta^2 = 1 \times 10^{-12}$, and $L/h = 50$ are plotted in Figs. 8 and 9, respectively. Clearly, the mode shapes change before and after the first and second crossing. Indeed, they keep moving with their uncoupled ($K = 0$ N/m) associated frequencies.

Similar to the plotted curves in Fig. 7, the effects of the linear stiffness coupling parameter (K) on the first four dimensionless transverse frequencies of FG CC–CC double nanobeams when $\eta^2 = 1 \times 10^{-12}$ and $L/h = 50$ are plotted in Fig. 10. It is shown from the plotted curves in Fig. 10 that, when increasing the stiffness coupling parameter, the changing of first four natural frequencies for the clamped–clamped configuration have the same trend as the simply supported configuration shown in Fig. 7. It should be mentioned that the required linear coupling stiffness for crossing becomes smaller when the power exponent increases. This can be explained by the linear softening behavior due to the increase in the power exponent. Compared to the simply supported beams configuration, it is clear that a higher value of the linear coupling stiffness is needed for the clamped configuration due to the hardening effect. Concerning the variations of the mode shapes before and after the first and second crossing, it follows from the plotted curves in Figs. 11 and 12 that the mode shapes are sensitive to the value of the linear coupling coefficient.

5.3 Vibration characteristics of triple connected FG nanobeams and importance of the linear coupling stiffness

The effects of the nonlocal parameter, linear coupling stiffness, and power exponent parameter on the coupled natural frequencies of triple connected FG nanobeams are deeply studied. In Fig. 13, the influence of the power

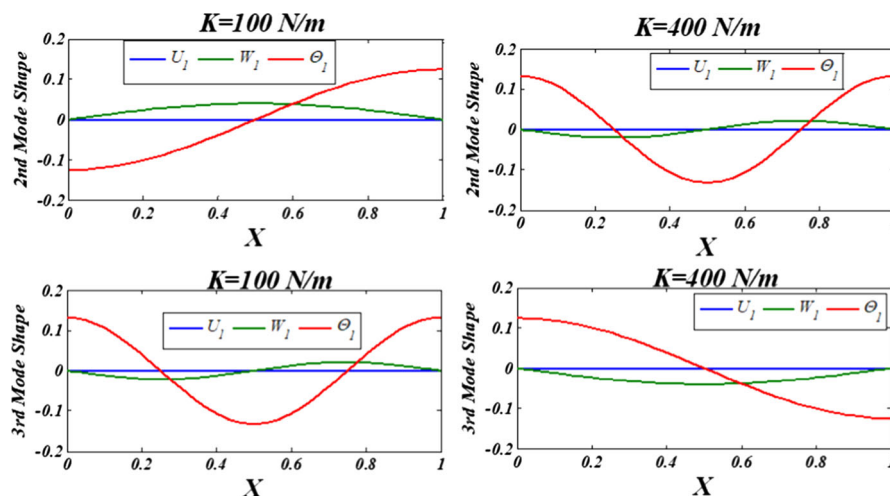


Fig. 8 The second and third mode shapes of nanobeam 1 with FG SS–SS ($k = 0$, $\eta^2 = 1 \times 10^{-12}$, $L/h = 50$) before and after the first crossing

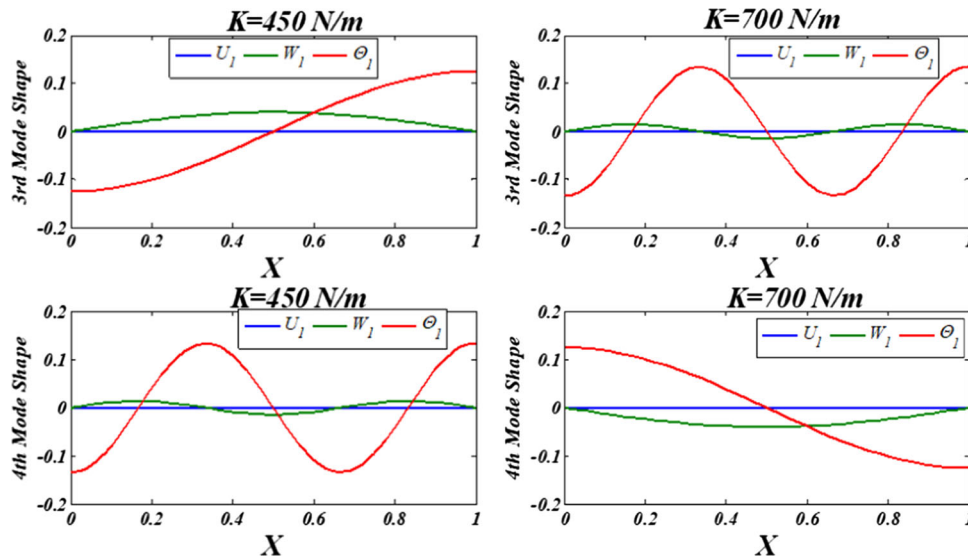
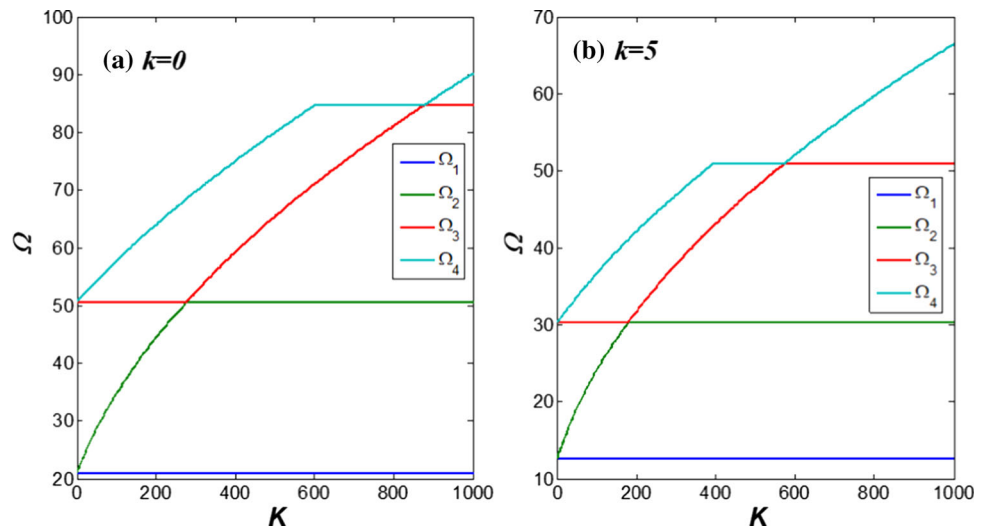


Fig. 9 The third and fourth mode shapes of nanobeam-1 with FG SS–SS ($k = 0, \eta^2 = 1 \times 10^{-12}, L/h = 50$) before and after the second crossing

Fig. 10 Variations of $\Omega_1, \Omega_2, \Omega_3,$ and Ω_4 as function of the stiffness parameter at different values of the power exponent for a FG CC–CC Timoshenko double nanobeam ($\eta^2 = 1 \times 10^{-12}, L/h = 50$)



exponent parameter (k) for four distinct values of the nonlocal parameter (η^2) on the first three dimensionless transverse frequencies of FG SS–SS–SS triple nanobeam when considering $K_1 = 1000 \text{ N/m}, K_2 = 10 \text{ N/m},$ and $L/h = 50$. The notation SS–SS–SS denotes that the three nanobeams are simply-supported at both boundaries. Inspecting the plotted curves in Fig. 13, it is obvious that both the power exponent and nonlocal elasticity parameters have softening properties on the natural frequencies, as predicted. Moreover, this figure reveals that the reduction of the frequencies is more remarkable for the higher modes. Further, the natural frequencies are in general more sensitive when k is in the range of $[0, 2]$.

To determine the effects of the nonlocal parameter on the first three natural frequencies, Fig. 14 is plotted when

considering FG SS–SS–SS triple nanobeams with $K_1 = 1000 \text{ N/m}, K_2 = 10 \text{ N/m},$ and $L/h = 50$. The nonlocal parameter is assumed to be varied in the interval $[0, 5 \times 10^{-12}]$. It follows from the plotted curves in Fig. 14 that the first two dimensionless transverse frequencies are less sensitive to the nonlocal parameter for this configuration of the linear coupling stiffnesses. It should be mentioned that the third natural frequency is sensitive than the lower frequencies to the nonlocal parameter and particularly when η^2 is in the range of $[0, 3 \times 10^{-12}]$.

It was showed in the previous section that the linear coupling stiffness between the nanobeams and the type of boundary conditions have significant impacts on the natural frequencies of the system. In Figs. 15 and 16, the coupling stiffness values are considered equal to each other ($K_1 = K_2 = 1000 \text{ N/m}$) in order to determine the influence

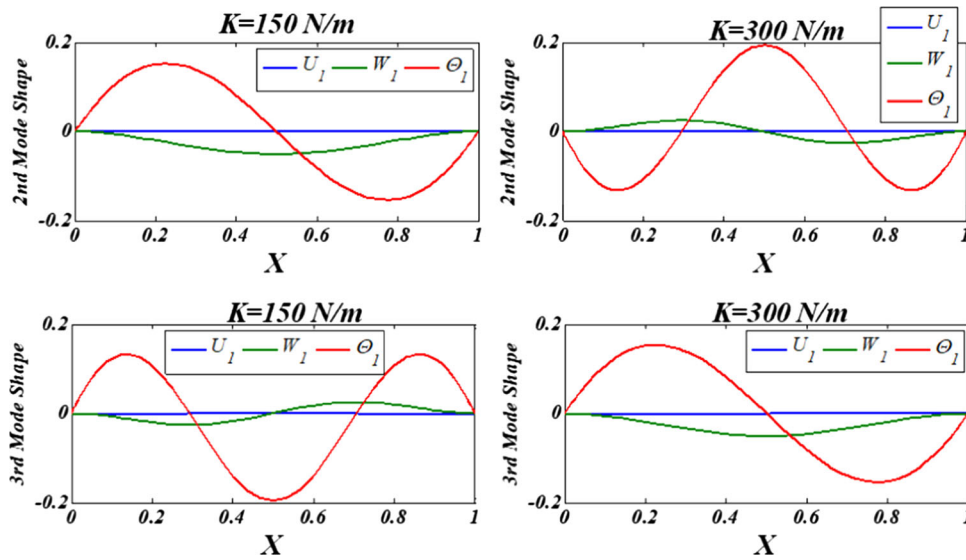


Fig. 11 The second and third mode shapes of nanobeam-1 with FG CC–CC ($k = 5, \eta^2 = 1 \times 10^{-12}, L/h = 50$) before and after the first crossing

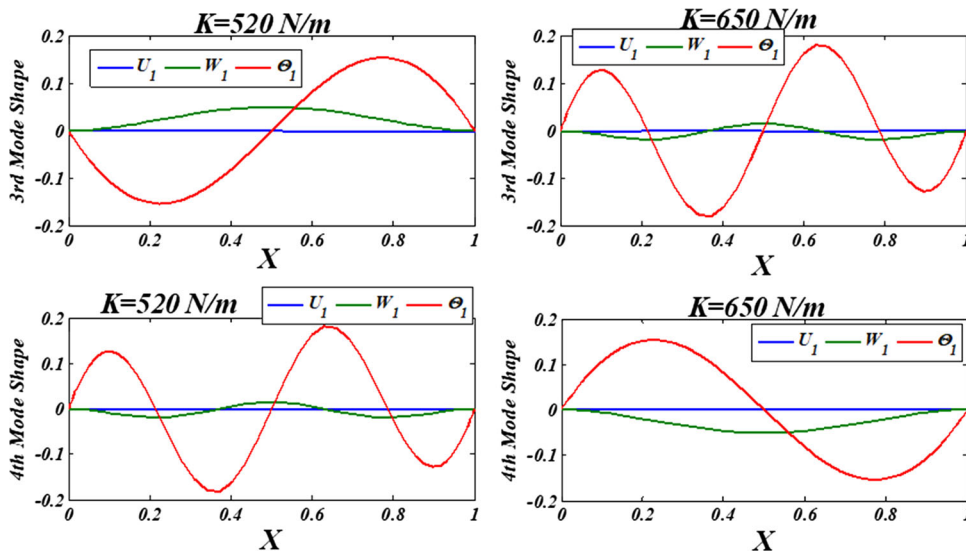


Fig. 12 The third and fourth mode shapes of nanobeam-1 with clamped edges ($k = 5, \eta^2 = 1 \times 10^{-12}, L/h = 50$) before and after the second crossing

of the power exponent and nonlocal parameters on the first three dimensionless transverse frequencies of FG CC–CC–CC triple nanobeam when $L/h = 50$. The notation CC–CC–CC indicates that the three nanobeams are clamped at both boundaries. As expected, the plots in Figs. 15 and 16 show that both k and η^2 parameters have a softening behavior on the transverse natural frequencies with a higher sensitivity to the power exponent parameter between zero and 4.

To investigate the impacts of the linear coupling stiffness on the system’s natural frequencies and existence of crossing of modes, the plotted curves in Fig. 17 display the effects of the stiffness parameter (K_1) at different values of

the power exponent (k) on the first four dimensionless transverse frequencies of FG SS–SS–SS triple nanobeams when considering $\eta^2 = 1 \times 10^{-12}, K_2 = 100 \text{ N/m}$, and $L/h = 50$. The plots in Fig. 17 indicates that the alteration of frequencies by increasing the linear stiffness coupling parameter do not have the same trend for different values of the power exponent of the FG material. The first dimensionless transverse frequency is not sensitive to the change of stiffness parameter (K_1). As for the second frequency, it increases with having a hardening effect in the linear coupling stiffness (K_1). As for the variations of the third and four natural frequencies, it is clear that the crossing between these two modes is strongly dependent on

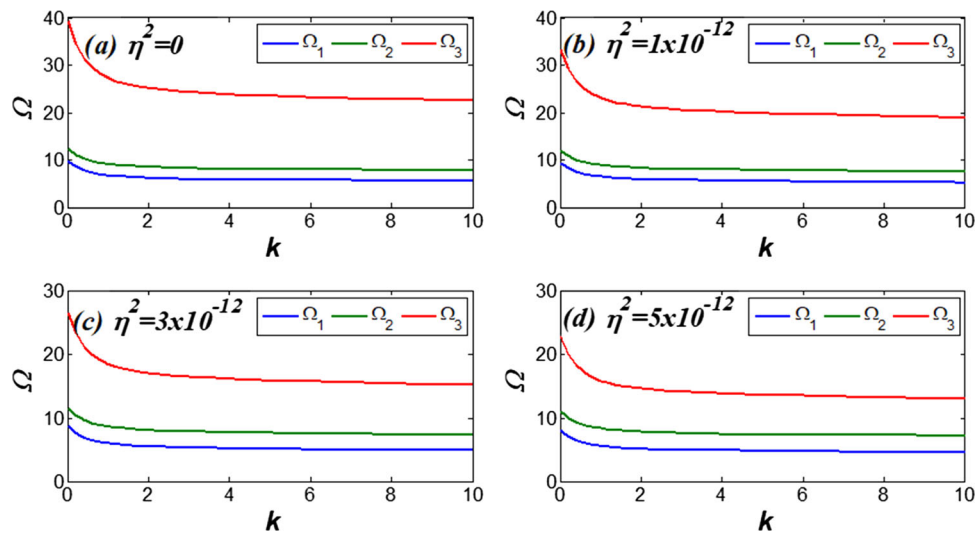


Fig. 13 Variations of the first three fundamental frequencies as function of the power exponent parameter at different values of the nonlocal parameter for a FG SS–SS–SS Timoshenko triple nanobeam ($K_1 = 1000 \frac{N}{m}, K_2 = 10 N/m, L/h = 50$)

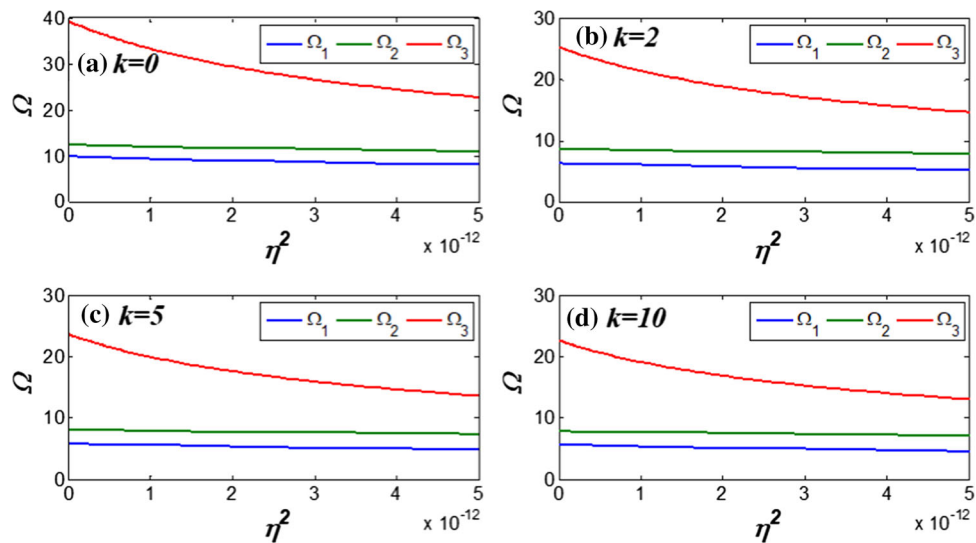


Fig. 14 Variations of the first three fundamental frequencies as function of the nonlocal parameter for various values of the power exponent parameter for a FG SS–SS–SS Timoshenko triple nanobeam ($K_1 = 1000 N/m, K_2 = 10 N/m, L/h = 50$)

the material degradation coefficient. In fact, when $k = 0$, the third frequency is first increased then by increasing the stiffness parameter (K_1), it is fixed. On the other hand, by increasing the power exponent to ($k = 5$), the third frequency is not sensitive to the increase in the linear stiffness coupling (K_1). While the fourth frequency is increased by increasing the stiffness parameter (K_1).

Figure 18 shows the mode shapes of third and fourth FG SS–SS–SS triple nanobeams for two distinct values of spring (K_1) before and after the crossing with ($K_2 = 100 N/m, k = 0, \eta^2 = 1 \times 10^{-12}, L/h = 50$). It follows from the plots in Fig. 18 that by increasing the value of the linear coupling spring, the third mode shape is

sensitive and change behavior, however, the fourth mode shape has the same response. Indeed, before the crossing, it is clear that the third mode is dominant by one of the beam’s first mode and the fourth mode is dominant by the second mode of another beam. After the crossing and for higher values of the linear coupling stiffness, both modes behave similarly with the characteristics of the second mode of two distinct beams. This can be explained by the existence of another crossing between the fifth and fourth modes which is not shown in Fig. 18.

Similar to the simply-supported boundary conditions, Fig. 19 display the effects of the stiffness parameter (K_1) at different values of the power exponent (k) on the first four dimensionless transverse frequencies of FG CC–CC–CC

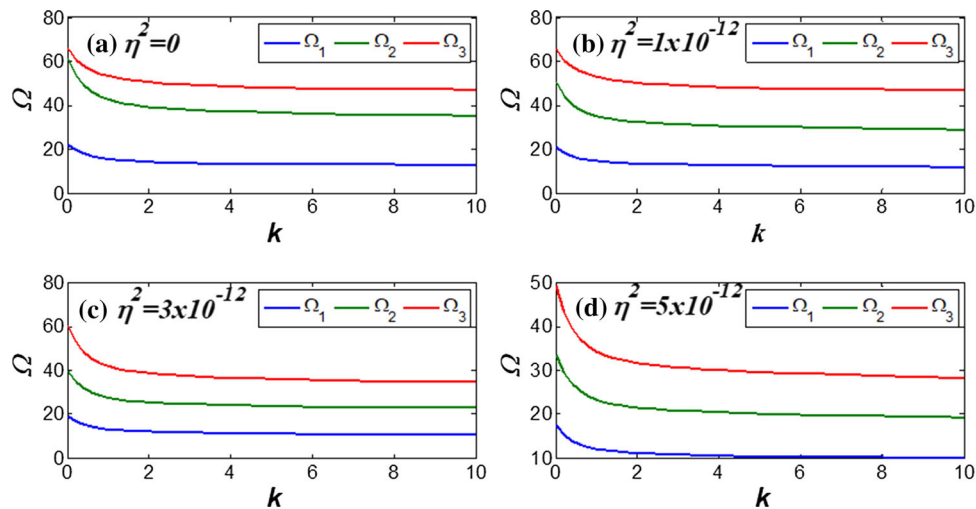


Fig. 15 Variations of the first three fundamental frequencies as function of the power exponent parameter at different values of the nonlocal parameter for a FG CC–CC–CC Timoshenko triple nanobeam ($K_1 = 1000\text{ N/m}$, $K_2 = 1000\text{ N/m}$, $L/h = 50$)

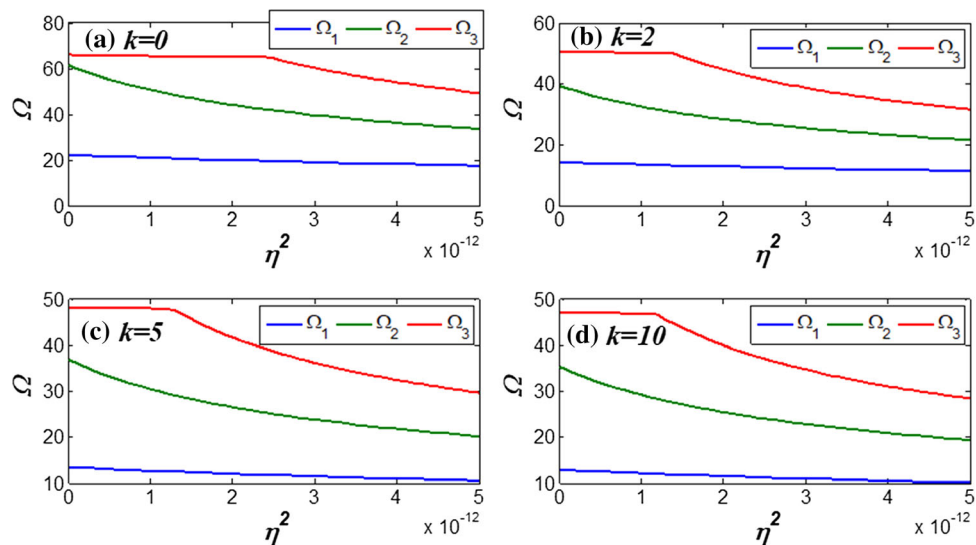


Fig. 16 Variations of the first three fundamental frequencies as function of the nonlocal parameter for various values of the power exponent parameter for a FG CC–CC–CC Timoshenko triple nanobeam ($K_1 = 1000\text{ N/m}$, $K_2 = 1000\text{ N/m}$, $L/h = 50$)

triple nanobeams when considering $\eta^2 = 1 \times 10^{-12}$, $K_2 = 100\text{ N/m}$, and $L/h = 50$. Inspecting the plotted curves in Fig. 19, it is obvious that the variation of frequencies by increasing the linear stiffness parameter (K_1) do not have the same trend for different values of the power exponent of the FG material compared to the simply supported configuration. The first dimensionless transverse frequency is not sensitive to the change of the stiffness parameter (K_1). The second frequency is increased by increasing the linear coupling stiffness parameter (K_1). The third nondimensional frequency is first increased by increasing the linear stiffness parameter and then it is not sensitive to the hardening effect of the linear spring. While the fourth nondimensional frequency is fixed and then

smoothly increased when linear spring parameter is increased. As shown in the double connected beam scenario, the power exponent increase results in a softening effect and hence lowering the required linear stiffness coupling coefficient for the crossing. Concerning the mode shapes variations before and after the crossing, Fig. 20 display the mode shapes of the third and fourth FG CC–CC–CC triple nanobeam-1 for two distinct values of spring (K_1). Similar to the results obtained in the simply supported configuration, the mode shapes are different before the crossing due to the activation of two different modes of distinct beams. However, after the crossing, the mode shapes are similar due to the interaction/crossing between

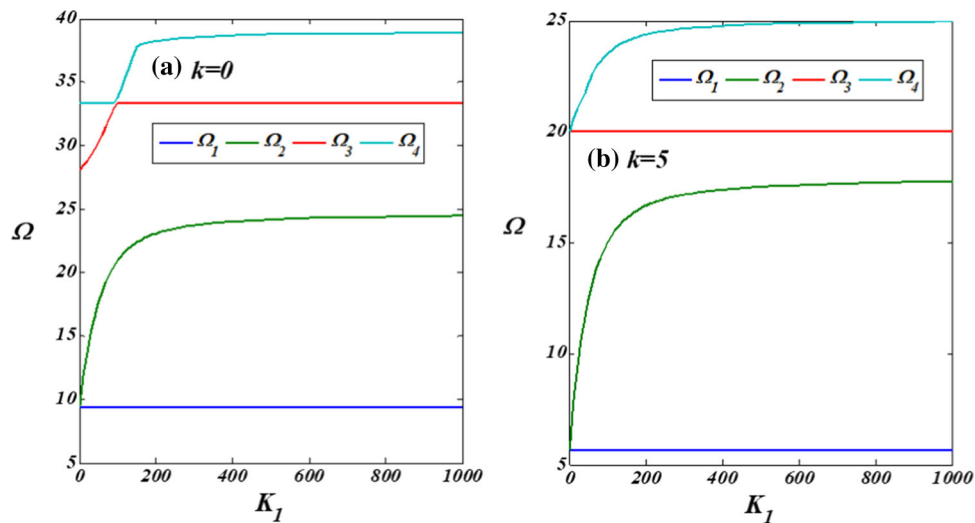


Fig. 17 Variations of $\Omega_1, \Omega_2, \Omega_3,$ and Ω_4 as function of the stiffness parameter K_I at different values of the power exponent for a FG SS–SS–SS Timoshenko triple nanobeams ($\eta^2 = 1 \times 10^{-12}, K_2 = 100 \text{ N/m}, L/h = 50$)

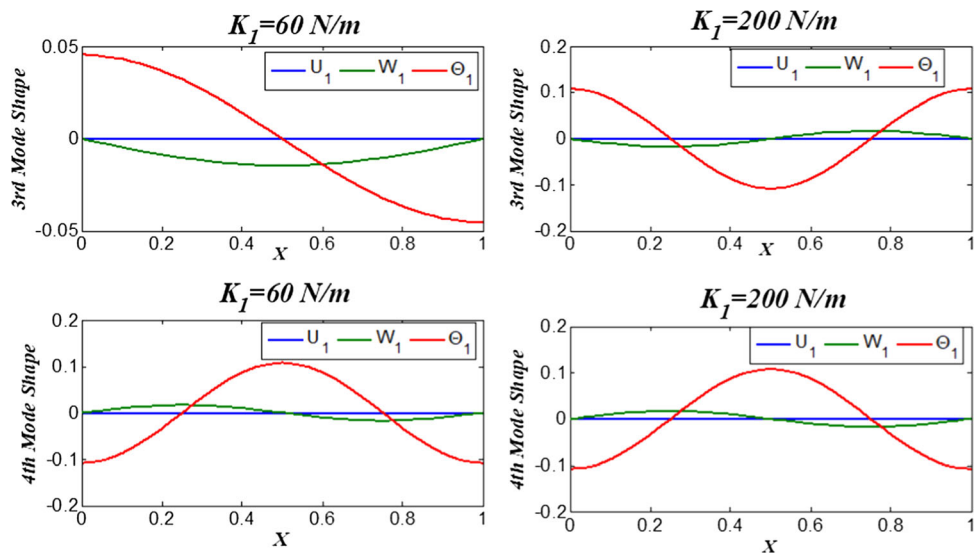


Fig. 18 The third and fourth mode shapes of nanobeam-1 with simply supported edges ($K_2 = 100 \text{ N/m}, k = 0, \eta^2 = 1 \times 10^{-12}, L/h = 50$).

the fourth and fifth modes and hence the activation of another second bending mode of a distinct beam.

6 Conclusions

The vibration properties of nonlocal FG double and multiple nanobeams were investigated. The multi-layered beams were modeled using the nonlocal Timoshenko beam theory, and it was assumed that they were connected by a continuous layer of linear springs. The Chebyshev spectral

collocation method was employed, and the partial differential governing equations of motion were converted into algebraic equations. Next, the boundary conditions were applied, and the eigenvalue problem was carried out to determine the dimensionless natural frequencies and their corresponding mode shapes. Then, the impacts of the nonlocal parameter, stiffness elastic medium, power exponent parameter, and number of connecting layers were deeply investigated. It was found that the power exponent parameter plays a major role in the magnitudes of the nondimensional natural frequencies. Increasing the power

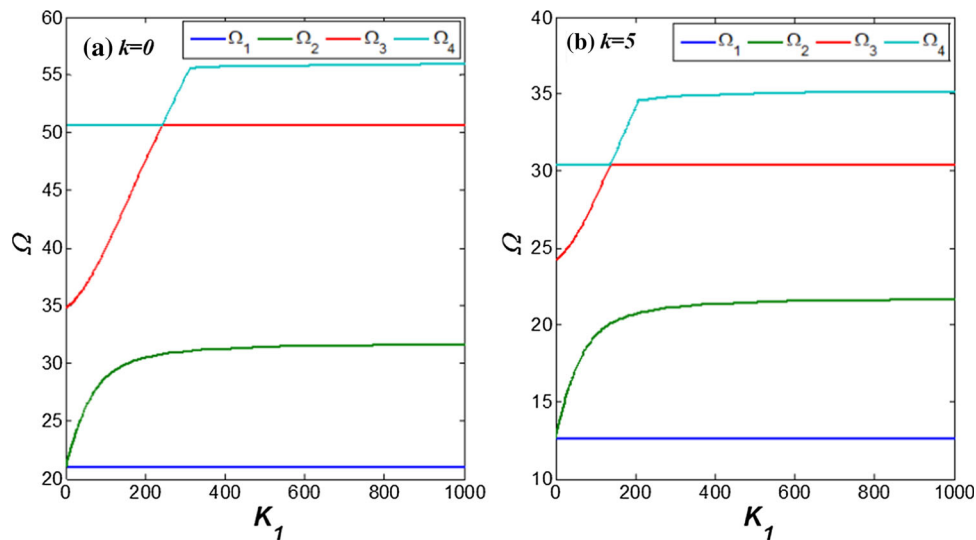


Fig. 19 Variations of Ω_1 , Ω_2 , Ω_3 , and Ω_4 as function of the stiffness parameter K_1 at different values of the power exponent for a FG CC–CC–CC Timoshenko triple nanobeam ($\eta^2 = 1 \times 10^{-12}$, $K_2 = 100 \text{ N/m}$, $L/h = 50$)

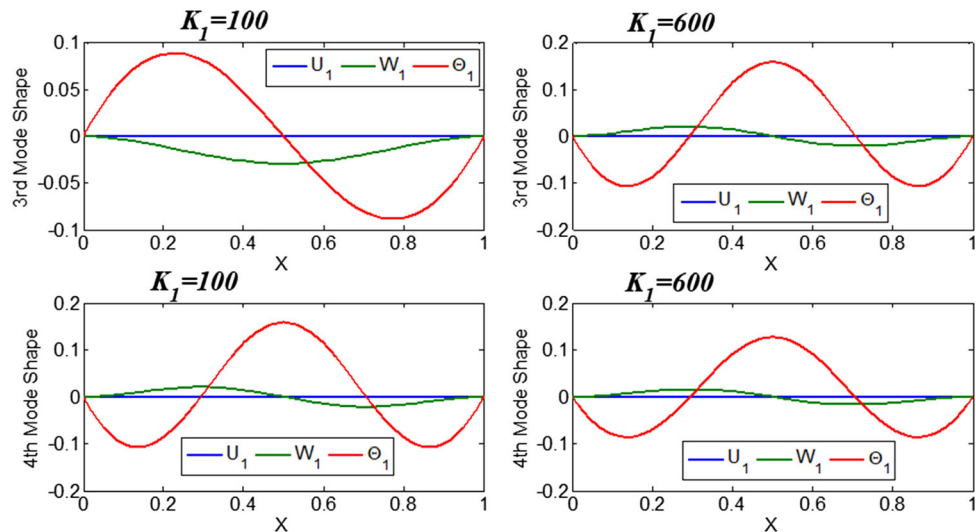


Fig. 20 The third and fourth mode shapes of nanobeam-1 with clamped edges ($K_2 = 100 \text{ N/m}$, $k = 5$, $\eta^2 = 1 \times 10^{-12}$, $L/h = 50$).

exponent parameter causes the natural frequencies to be reduced. Moreover, the results indicated that the nonlocal parameter significantly impacts the natural frequencies by resulting in a softening effect. It was showed that the crossing phenomenon can take place depending on the linear coupling stiffness between the layers, the nonlocal parameter, and the power exponent. This analysis showed the importance of accurately modeling and studying the vibration properties of multi-layered nanobeams.

Compliance with ethical standards

Data availability The raw/processed data required to reproduce these findings cannot be shared at this time due to time limitations.

References

- Aranda-Ruiz J, Loya J, Fernández-Sáez J (2012) Bending vibrations of rotating nonuniform nanocantilevers using the Eringen nonlocal elasticity theory. *Compos Struct* 94(9):2990–3001
- Arash B, Wang Q (2011) Vibration of single-and double-layered graphene sheets. *J Nanotechnol Eng Med* 2(1):7
- Ball P (2001) Roll up for the revolution. *Nature* 414:142. <https://doi.org/10.1038/35102721>
- Baughman RH, Zakhidov AA, De Heer WA (2002) Carbon nanotubes—the route toward applications. *Science* 297(5582):787–792
- Bodily BH, Sun CT (2003) Structural and equivalent continuum properties of single-walled carbon nanotubes. *Int J Mater Prod Technol* 18(4–6):381–397
- Chen J, Guo J, Pan E (2017) Wave propagation in magneto-electro-elastic multi-layered plates with nonlocal effect. *J Sound Vib* 400:550–563

- Eringen AC (1983) On differential equations of nonlocal elasticity and solutions of screw dislocation and surface waves. *J Appl Phys* 54(9):4703–4710
- Eringen AC (2002) *Nonlocal continuum field theories*. Springer Science & Business Media
- Eringen AC (2006) Nonlocal continuum mechanics based on distributions. *Int J Eng Sci* 44(3–4):141–147
- Ghadiri M, Shafiei N (2016) Nonlinear bending vibration of a rotating nanobeam based on nonlocal Eringen's theory using differential quadrature method. *Microsyst Technol* 22(12):2853–2867
- Guo J, Chen J, Pan E (2018) A three-dimensional size-dependent layered model for simply-supported and functionally graded magneto-electroelastic plates. *Acta Mech Solida Sin* 31(5):652–671
- Hashemi SH, Khaniki HB (2018) Dynamic response of multiple nanobeam system under a moving nanoparticle. *Alexandria Eng J* 57(1):343–356
- Karličić D, Cajić M, Adhikari S (2018) Dynamic stability of a nonlinear multiple-nanobeam system. *Nonlinear Dyn* 93(3):1495–1517
- Khaniki HB (2018a) On vibrations of nanobeam systems. *Int J Eng Sci* 124:85–103
- Khaniki HB (2018b) Vibration analysis of rotating nanobeam systems using Eringen's two-phase local/nonlocal model. *Phys E* 99:310–319
- Lam DC, Yang F, Chong ACM, Wang J, Tong P (2003) Experiments and theory in strain gradient elasticity. *J Mech Phys Solids* 51(8):1477–1508
- Li C, Chou TW (2003) A structural mechanics approach for the analysis of carbon nanotubes. *Int J Solids Struct* 40(10):2487–2499
- Li X, Guo J, Sun T (2019a) Bending deformation of multi-layered one-dimensional quasicrystal nanoplates based on the modified couple stress theory. *Acta Mech Solida Sin* 32(6):785–802
- Li C, Guo H, Tian X, He T (2019b) Size-dependent thermo-electromechanical responses analysis of multi-layered piezoelectric nanoplates for vibration control. *Compos Struct* 225:111112
- Liu JC, Zhang YQ, Fan LF (2017) Nonlocal vibration and biaxial buckling of double-viscoelastic-FGM-nanoplate system with viscoelastic Pasternak medium in between. *Phys Lett A* 381(14):1228–1235
- Ma'een SS, Ceballes S, Abdelkefi A (2018) Nonlocal buckling analysis of functionally graded nano-plates subjected to biaxial linearly varying forces. *Microsyst Technol* 24(4):1935–1948
- Murmu T, Adhikari S (2010a) Nonlocal transverse vibration of double-nanobeam-systems. *J Appl Phys* 108(8):083514
- Murmu T, Adhikari S (2010b) Nonlocal effects in the longitudinal vibration of double-nanorod systems. *Phys E* 43(1):415–422
- Murmu T, Adhikari S (2011) Axial instability of double-nanobeam-systems. *Phys Lett A* 375(3):601–608
- Murmu T, Pradhan SC (2009) Small-scale effect on the vibration of nonuniform nanocantilever based on nonlocal elasticity theory. *Phys E* 41(8):1451–1456
- Murmu T, Sienz J, Adhikari S, Arnold C (2013) Nonlocal buckling of double-nanoplate-systems under biaxial compression. *Compos B Eng* 44(1):84–94
- Rahmani O, Pedram O (2014) Analysis and modeling the size effect on vibration of functionally graded nanobeams based on nonlocal Timoshenko beam theory. *Int J Eng Sci* 77:55–70
- Reddy JN (2007) Nonlocal theories for bending, buckling and vibration of beams. *Int J Eng Sci* 45(2–8):288–307
- Reddy JN (2010) Nonlocal nonlinear formulations for bending of classical and shear deformation theories of beams and plates. *Int J Eng Sci* 48(11):1507–1518
- Reddy JN, El-Borgi S (2014) Eringen's nonlocal theories of beams accounting for moderate rotations. *Int J Eng Sci* 82:159–177
- Roque CMC, Ferreira AJM, Reddy JN (2011) Analysis of Timoshenko nanobeams with a nonlocal formulation and meshless method. *Int J Eng Sci* 49(9):976–984
- Sari MES, Butcher EA (2011) Three dimensional vibration analysis of rectangular plates with undamaged and damaged boundaries by the spectral collocation method. In: ASME 2011 international design engineering technical conferences and computers and information in engineering conference. American Society of Mechanical Engineers Digital Collection, pp 37–45
- Sari ME, Shaat M, Abdelkefi A (2017) Frequency and mode veering phenomena of axially functionally graded non-uniform beams with nonlocal residuals. *Compos Struct* 163:280–292
- Sari S, Al-Kouz GW, Atieh MA (2020) Transverse vibration of functionally graded tapered double nanobeams resting on elastic foundation. *Appl Sci* 10(2):493
- Shaat M, Abdelkefi A (2017) New insights on the applicability of Eringen's nonlocal theory. *Int J Mech Sci* 121:67–75
- Şimşek M (2011) Nonlocal effects in the forced vibration of an elastically connected double-carbon nanotube system under a moving nanoparticle. *Comput Mater Sci* 50(7):2112–2123
- Sun J, Zhao J, Gong F, Li Z, Ni X (2018) Design, fabrication and characterization of multi-layer graphene reinforced nanostructured functionally graded cemented carbides. *J Alloy Compd* 750:972–979
- Thai HT (2012) A nonlocal beam theory for bending, buckling, and vibration of nanobeams. *Int J Eng Sci* 52:56–64
- Trefethen LN (2000) *Spectral methods in MATLAB*, vol 10. Siam
- Wang CM, Zhang YY, He XQ (2007) Vibration of nonlocal Timoshenko beams. *Nanotechnology* 18(10):105401
- Yang FACM, Chong ACM, Lam DCC, Tong P (2002) Couple stress based strain gradient theory for elasticity. *Int J Solids Struct* 39(10):2731–2743

Publisher's Note Springer Nature remains neutral with regard to jurisdictional claims in published maps and institutional affiliations.